

A novel method to detect circulating antigens of *Schistosoma japonicum* using a gold nanorod optical sensor

He, X.¹, Wang, S.P.^{1*}, Zhou, Y.F.¹, Huang, C.M.¹, Ning, S.B.¹ and LvQ, S.J.¹

¹Department of Parasitology, Xiangya School of Medicine, Central South University, Changsha, 410078, PR China

*Corresponding author e-mail: spwang@126.com.

Received 13 May 2016, received in revised form 1 October 2016; accepted 2 October 2016

Abstract. Diagnostic method of *Schistosoma japonicum* (*S.japonicum*) is the key of schistosomiasis prevention and control. In China, schistosomiasis reached the stage of transmission control, and almost of the epidemic areas tend to have low infection rate and intensity, but it is difficult for the existing detection methods to achieve accurate monitoring. In this study, a novel method to detect the circulating antigens of *S.japonicum* using gold nanorods optical sensor was developed. Gold nanorods were prepared by seed-mediated growth followed by deposition onto Indium-Tin-Oxide (ITO) glass to fabricate a solid phase biosensor. In order to assembly between the ITO glass and gold nanorod, hydroxylation and sulfhydrylation were carried out to modify the ITO glass. Surface of gold nanorods was conjugated with an SIEA26-28kDaSjScFv antibody against *S.japonicum* circulating antigens, and the sensor optical changed upon antigen-antibody recognition. The sensor was used to detect *S.japonicum* infection in rabbits by testing the serum once a week for 8 weeks. Results revealed different displacement of localized surface plasmon resonance (LSPR) of the gold nanorod optical sensor each week while the control group showed no such change in LSPR. Simultaneously, Indirect Hemagglutination Assay (IHA) and Fast Enzyme-Linked Immuno Sorbent Assay (F-ELISA) method were used to test these samples. Ten human serum samples from *S.japonicum* infected patients were analyzed using the gold nanorods optical sensor, which revealed that health human serum did not show any spectrum displacement. We developed a specificity gold nanorod optical sensor by combining the SIEA26-28kDaSjScFv, which was used to detect circulating antigens of *S.japonicum*. This method is expected to overcome the issues pertaining to the testing of circulating antigens of *S.japonicum*.

INTRODUCTION

Schistosoma japonicum (*S.japonicum*) is the causative agent of one of the most serious zoonotic infections, schistosomiasis, and is mainly present in Africa, Asia, and America. In China, the infection ratio in endemic areas have been declining, and the severity of infection, expressed as eggs per gram (EPG), have also been decreasing due to early diagnosis and therapy. Monitoring the source is important to control infection and block transmission, and sensitive diagnostic methods are essential to detect the presence

of mild *S.japonicum* infection in patients and animals. The feces detection method was recognized as the “gold standard” for detecting *Schistosoma* by the World Health Organization (WHO), but the method is unable accurately to detect eggs in the feces when individuals have a low degree of *Schistosoma* infection (Kongs *et al.*, 2001). And immunological methods are sensitive and specific, but the efficacy of these methods are affected by factors such as changes in antibody levels with the ebb and flow of symptoms (Chitsulo *et al.*, 2004). Thus, there is need to develop a new detection

method for schistosomiasis. Recently, researchers reported that *Schistosoma* circulating antigen could be used as a marker of infection and as an indicator of the presence of living worms, or for the assessment of recovery (Legesse *et al.*, 2008; Lei *et al.*, 2012). Moreover, international and domestic research facilities are currently studying *S.japonicum* circulating antigen (SjCag) extensively and are exploring the antigen properties, source analysis, and other parameters (Lu *et al.*, 2012; Cai *et al.*, 2014). However, the level of circulating antigen is too low in blood to be detected by conventional immunological methods. Hence, developing a sensitive method that can detect SjCag and diagnose infected patients is imperative.

Nanomaterials have many fundamental uses and applications in medical research. Especially, gold nanorod optical sensors are generally valued and applied to many fields (Chen *et al.*, 2007; Mayer & Hafner, 2011; Shalabney & Abdulhalim, 2012; Szunerits *et al.*, 2013). Sensitivity of detection can be increased by adapting these sensors for the detection of antigens. Gold nanorods (GNRs) have received much attention due to their unique optical properties that are dependent on their shape, size, aspect ratio and so on. In this study, construction and assembly of gold nanorod optical sensors conjugated to the SIEA26-28kDaSjScFv antibody was performed for early diagnosis of *S.japonicum* by measuring circulating antigen. In recent research, the use of gold nanorods for detecting biological interactions between antigens and antibodies is still in its infancy.

Our group has established many immune sensor methods to detect the *S.japonicum* antigen (Liu *et al.*, 2001; Wu *et al.*, 2003; Chu *et al.*, 2005; Wen *et al.*, 2011; Wang *et al.*, 2012). Based on above researches, we constructed a gold nanorods optical sensor and conjugated it to the SIEA26-28kDaSjScFv antibody, which can detect the circulating antigen of *S.japonicum*.

Materials

Gold chloride trihydrate ($\text{HAuCl}_4 \cdot 3\text{H}_2\text{O}$) and cetyltrimethylammonium bromide (CTAB) were purchased from Amresco LLC (Solon, OH, U.S.A); sodium borohydride (NaBH_4) was purchased from Tianjin Chemical Reagent Research Institute Co., Ltd. (Tianjin, China); silver nitrate was purchased from Sinopharm Chemical Reagent Co., Ltd. (Shanghai, China); L-ascorbic acid, poly(sodium 4-styrenesulfonate) (PSS), poly(allylamine hydrochloride) (PAH), and (3-mercaptopropyl) trimethoxysilane (MPTMS) were purchased from Sigma Aldrich (Shanghai, China); ITO glass (7 mm×50 mm×1 mm) was purchased from South China Xiang Cheng Technology Co., Ltd. (Shenzhen, China).

Animal serum sample

New Zealand rabbits were supplied by the laboratory animal division of Central South University. Eight group rabbits were infected with 500 units of schistosome cercaria respectively, and 3-5 mL serum each rabbit was collected each week for 8 weeks, then stored at -30°C until further use.

Human serum sample

Human serum was collected from patients infected with *S.japonicum* from HuBei province in China. Gold nanorod optical sensors was used to analyze 10 human serum samples. Health human serum was used as a control group.

Preparing SIEA26-28kDaSjScFv antibody

SIEA26-28kDaSjScFv was previously prepared by our group (Gao *et al.*, 2010). Expression of the recombinant plasmid was seen under optimal conditions, and the antibody was stored for future use.

Preparation of gold nanorod

Gold nanorod was prepared by seed-mediated growth. Briefly, seed solution: $\text{HAuCl}_4 \cdot 3\text{H}_2\text{O}$ (0.01 M) was added to CTAB (0.1 M) in a test tube. Subsequently, NaBH_4 (0.01 M) was added, followed by magnetic stirring for 3 min. The solution developed a brownish colour. The test tube was then incubated at 25°C for 2 h. Next, $\text{HAuCl}_4 \cdot 3\text{H}_2\text{O}$ (0.01 M) was mixed with CTAB (0.1 M), then AgNO_3 (0.01 M) and L-ascorbic acid (0.01 M) were added to the solution in sequence. The solution became colourless immediately upon the addition of L-ascorbic acid. Finally, 0.01 mL of the seed solution was added and the mixture was incubated at 25°C for a minimum of 3 h.

In order to keep the solution stable, it was necessary to remove excess CTAB and add Cl^- ions in gold nanorods solution. First, the solution of gold nanorods was centrifuged at 8500 rpm ($5023 \times g$) for 30 min. The supernatant was carefully discarded and 1 mL deionized water ($18.2 \Omega\text{-cm}$) was added to each tube to redisperse the nanoparticle pellet. The solution was then centrifuged at 14,000 rpm ($13,628 \times g$) for 15 min. The supernatant was discarded and 1 mL CTAB (0.5 mM) was added into the tube to redisperse the gold nanorods. The solution was centrifuged again. The supernatant was discarded and 1 mL NaCl (5 mM) was added to the solution (Wang & Tang, 2013).

Biosensor assembly

The ITO substrates were immersed into piranha solution ($98\% \text{H}_2\text{SO}_4 : 30\% \text{H}_2\text{O}_2 = 3:1$ v/v) and boiled for 25 min. The slides were then incubated in piranha solution for 40 min at 70°C . After hydroxylation, ITO substrates were divided into two groups. The first group was immersed into MPTMS solution for the sulfhydrylation overnight at 4°C , and the other one as a control group was used without any further treatment. Finally, all of the ITO glass slides were immersed into the gold nanorods solution for 16 h at 25°C . In order to enhance the sensitivity of the sensor, we changed the surface charge of GNRs by immersing the ITO glasses into PSS (2 mg/mL) and PAH (2 mg/mL) solutions for 30 min each, respectively.

Optimization assembly condition

In order to improve conjugation between the biosensor and antibody, condition of the biosensor and antibody were optimized by assembly time and antibody concentration. First, ITO glass was immersed into SIEA26-28kDaSjscFv solution for 0.5 h, 2 h, 4 h, 6 h, and 16 h at 25°C , then results were recorded. Second, optimal antibody concentration for assembly was analyzed by measuring localized surface plasmon resonance (LSPR) displacement of the sensor. PBS (pH 7.4) was used to dilute SIEA26-28kDaSjscFv 1:5, 1:10, and 1:20 respectively, followed by reaction with ITO glass for 2 hours at 4°C . BCA protein assay kit was used according to manufacturer's instructions to detect SIEA26-28kDaSjscFv concentration of the different dilutions. The absorbance of the solution was detected by a microplate reader at a wavelength of 562 nm, and then to calculate the concentration of SIEA26-28kDaSjscFv.

Analysis of infected serum

The infected rabbit serum samples were analyzed by gold nanorods optical sensor. In parallel, IHA and F-ELISA assays were performed as reference groups. In addition, the serum of patient infected with *S. japonicum* was analyzed.

Rabbit serum samples from each time point were incubated with the sensors conjugated with SIEA26-28kDaSjscFv at 4°C for 2 h. For the IHA test, manufacturer instructions were followed for the IHA kit (product NO.:3400632). Briefly, rabbit serum samples were diluted 1:5, 1:10, 1:20 and 1:40. The positive, negative, and blank control groups were also analyzed at 37°C for 30 min. For the F-ELISA analysis, briefly, serum samples were diluted 1:10, and positive, negative, blank control groups were also prepared. Samples were analyzed and the results were obtained by microplate reader at a wavelength of 490 nm. The detection threshold value of the positive control was 2.1 times greater than the control value (Bergquist 1992).

RESULTS

Preparing the gold nanorod

In this study, we prepared GNRs by seed-mediated growth. As shown in Fig. 1, the LSPR of GNRs showed a transverse plasmon resonance peak at 528 nm and a longitudinal resonance peak at 763 nm. TEM image showed the rod shape with a length of 36 ± 6 nm and a width of 11 ± 2 nm, resulting in an average aspect ratio of 3.2 (Fig. 2).

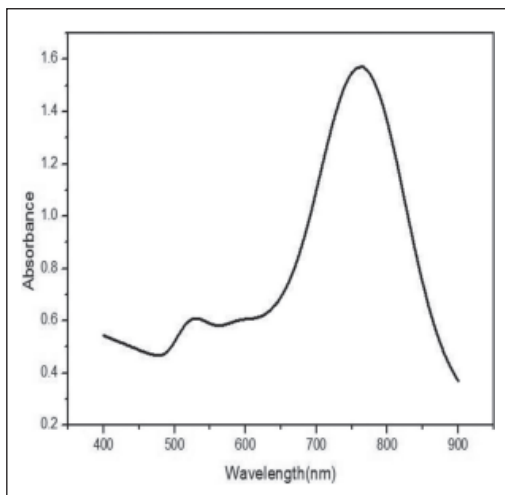


Figure 1. UV-Vis absorption spectrum of chemically synthesized gold nanorods showing a transverse surface plasmon resonance peak at 528 nm and a longitudinal resonance peak at 763 nm.

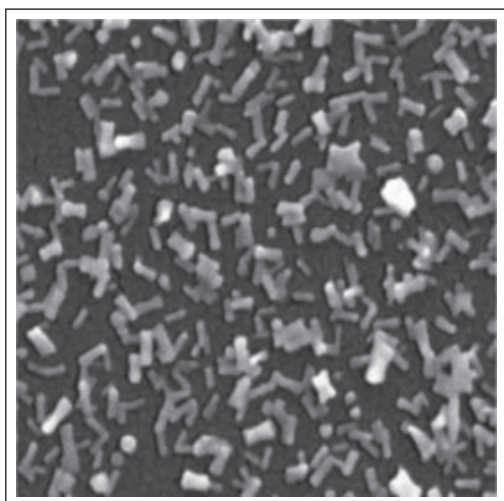


Figure 3. SEM images of gold nanorods coverage on the surface of ITO glass.

Biosensor assembly and optimization

Piranha solution and MPTMS were used as chemical modification reagents for the hydroxylation and sulfhydrylation of ITO glass respectively. TEM was used to confirm that the gold nanorods were assembled with the ITO glass (Fig. 3). In addition, the LSPR spectrum of the biosensor shows a displacement of the longitudinal resonance peak at 19 nm when combine the SIEA26-28kDaSjscFv (Fig. 4).

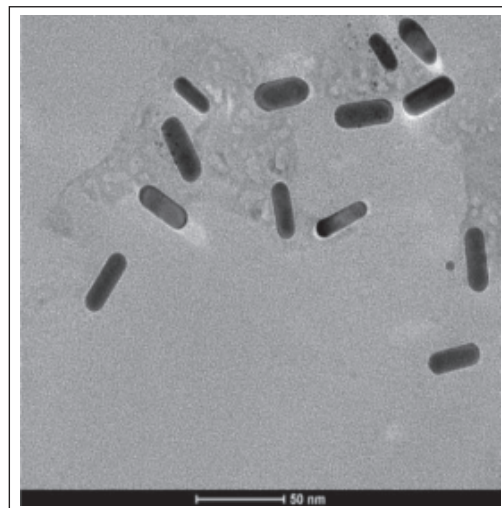


Figure 2. TEM image of monodispersed GNRs in solution.

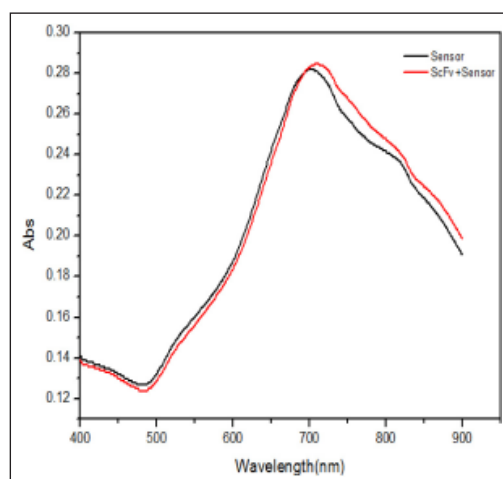


Figure 4. UV-Vis absorption spectra of nanosensors combined with SIEA26-28DaSjscFv before and after GNRs assembly on ITO glass substrate.

Through random selection, a detection point from the ITO glass was chosen and Energy Dispersive X-ray spectroscopy(EDX) analyzed (Fig. 5). The results showed that the sensors included Si, Au, O, S and some microelements which were expected (Fig. 6).

The connection between the gold nanorod and ITO glass determines the stability of the sensor. In the study, MPTMS was used as a sulfhydrylation reagent to modify the ITO glass, leading to ITO glass with SH groups which can covalently bond to gold nanorods. When the ITO glass lacks SH groups, the GNRs can still combined with the ITO glass (Fig. 7 a1), but they easily move out of the ITO-glass after 20 min (Fig. 7 a2). After 1 h, the GNRs were completely detached from ITO glass (Fig. 7 a3). LSPR spectra can also be used to provide evidence for this phenomenon (Fig. 7 b). Immediately after the GNRs assemble on the ITO glass, the LSPR spectra show an obvious peak, and after 20 min, the sample do not display any LSPR spectra; In contrast, GNRs can be tightly adsorbed onto the surface of ITO glass with SH group (Fig. 7c). The results of LSPR spectra are consistent with above results (Fig. 7d). GNRs were combined with ITO-glass by the Au-S covalent bonds, and the forces between the PSS and PAH was electrostatic. Hence, the covalent bonds formed after MPTMS treatment are crucial for detection of *SjC*Ag in serum.

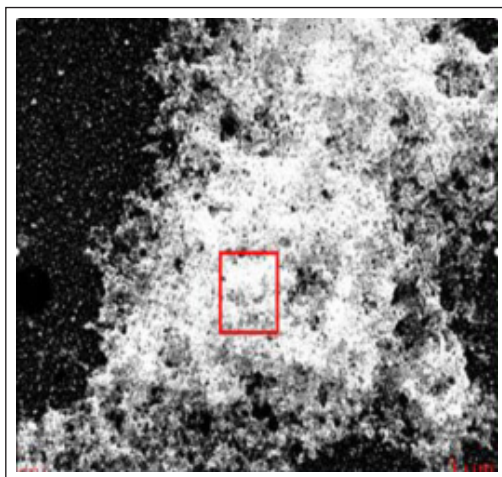


Figure 5. Randomly selected detection point.

Envelope of SIEA26-28kDaSjScFv

SIEA26-28kDaSjScFv can specifically recognize *SjC*Ag. The SIEA26-28kDaSjScFv stock solution was diluted 1:5, 1:10, and 1:20 with PBS(PH 7.4). A standard curve was used to calculate the concentration of SIEA26-28kDaSjScFv. The results were 2.596 mg/mL, 1.669 mg/mL, and 1.274 mg/mL for the dilutions, respectively (Fig. 8). The ITO glass slides were immersed into the SIEA26-28kDaSjScFv solution with different dilution for 2 h at 4°C. The longitudinal wave had a red shift of 23 nm, 21 nm, and 21 nm, respectively (Fig. 9). From the results, the SIEA26-28kDaSjScFv with the 1:5 (C=2.596 mg/mL) dilution ratio gave the largest shift .

Analysis of the change in the plasma resonance spectra of the sensors was performed by observing the spectra change after incubation of SIEA26-28kDaSjScFv antibody for different times point at 25°C, and get the best assembly time (Fig. 10). The results showed that a wavelength change from 679 nm to 703 nm up to 2 hours, and after 2 hours the wavelength movement had not significantly shifted further, such as 704 nm (4 h), 708 nm (6 h), 707 nm (16 h).

Detection of serum sample for different periods

Infected rabbits' serum samples were analyzed by GNRs sensor. The results showed that there were different displacement of

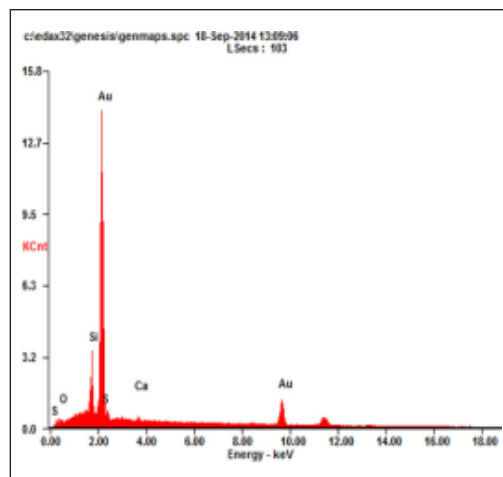


Figure 6. Energy Dispersive X-ray spectroscopy (EDX) analysis of gold nanorod sensors.

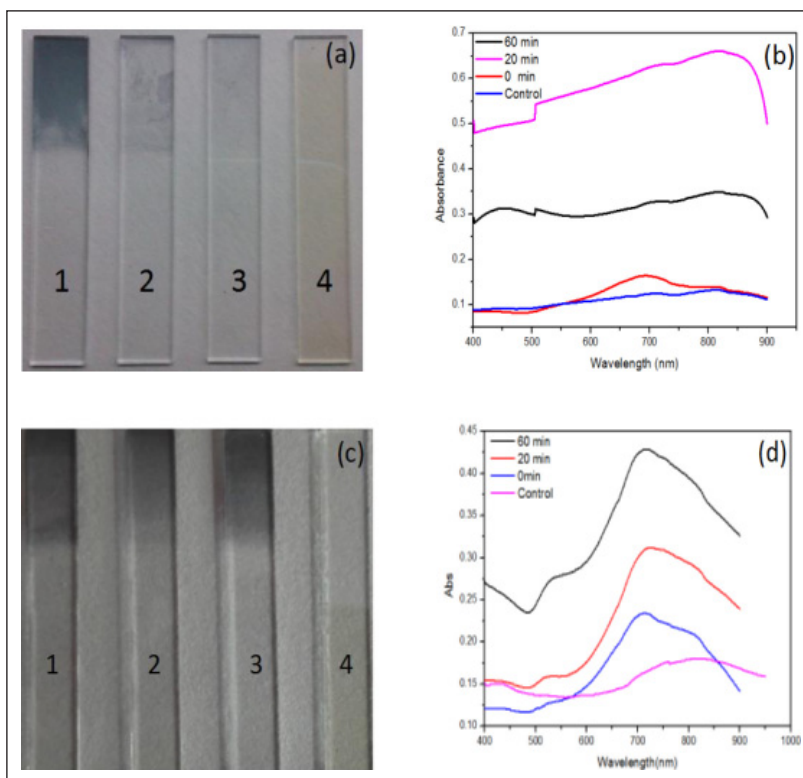


Figure 7. (a) The color change of ITO glass surfaces without SH groups at different times after combination with PSS/PAH solution. (a1) shows GNRs deposited on glass, (a2) is combine with PSS/PAH after 20 min, (a3) is combine with PSS/PAH after 60 min, and (a4) is ITO glass (Control). (b) UV-Vis absorption spectra of nanosensors without SH groups at different times after combination with PSS/PAH. (c) The color change of ITO glass surfaces with SH groups at different times after combination with PSS/PAH solution. (c1) shows GNRs deposited on ITO-glass, (c2) is combine with PSS/PAH after 20 min, (c3) is combine with PSS/PAH after 60 min, and (c4) is ITO glass (Control). (d) UV-Vis absorption spectra of nanosensors with SH groups at different times after combination with PSS/PAH.

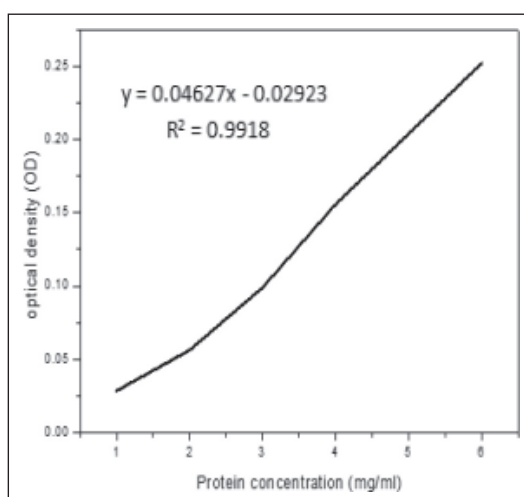


Figure 8. BCA standard protein curve.

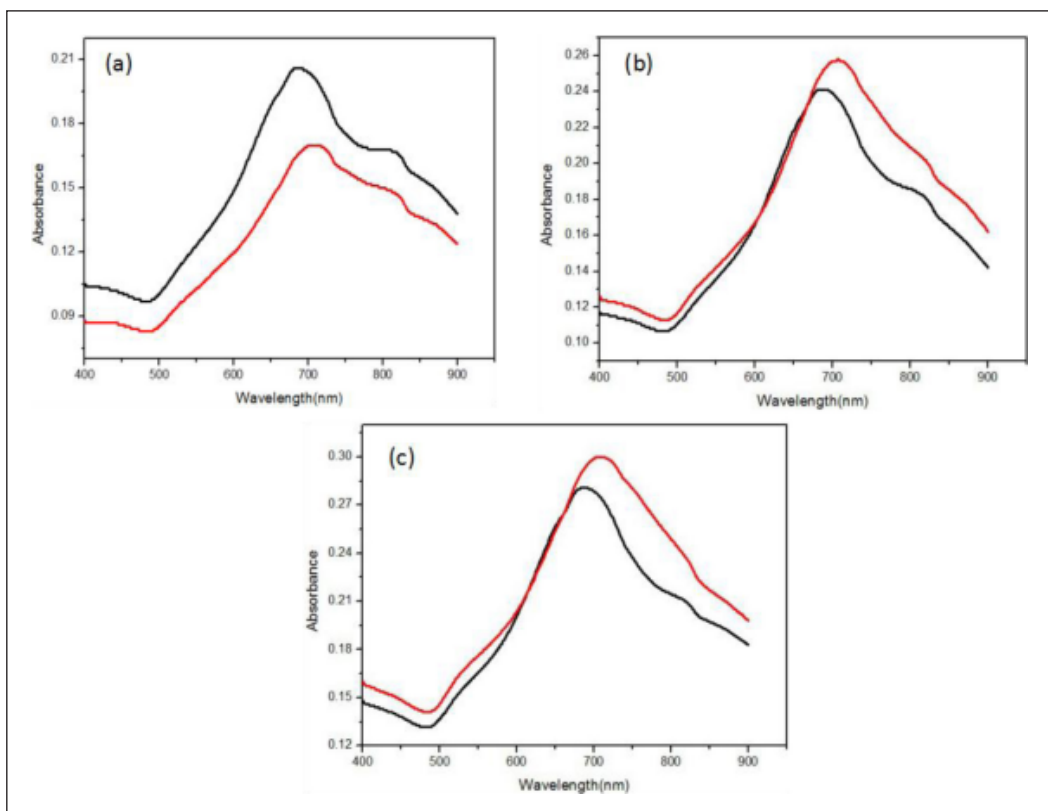


Figure 9. Comparison of the absorption spectra of nanosensors with different concentrations of SIEA26-28 kDa-*SjscFv*, Black and red curves represent the images before and after combination with SIEA26-28 kDa-*SjscFv*, respectively. (a) SIEA26-28 kDa-*SjscFv* concentration was 2.596 mg/mL and showed a red shift of 23 nm; (b) SIEA26-28 kDa-*SjscFv* concentration was 1.669 mg/mL and showed a red shift of 21 nm, (c) SIEA26-28 kDa-*SjscFv* concentration was 1.274 mg/mL and showed a red shift of 21 nm.

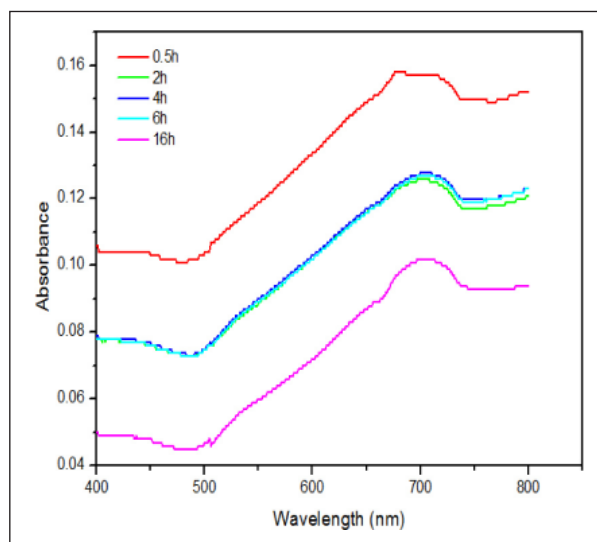


Figure 10. Change in UV-Vis absorption spectrum of sensor after assembly with SIEA26-28 kDa-*SjscFv* at different times.

LSPR wavelength, which was due to the antigen in the positive serum interacted with SIEA26-28kDaSjscFv antibody. Weekly samples from weeks 1-8 of infection showed shifts of 12 nm, 15 nm, 27 nm, 5 nm, 40 nm, 45 nm, 53 nm, 57 nm respectively (Fig. 11). Then, with increasing infection time, the wavelength shift occurred as followed: the change increase first, then dropped ,then finally increased again, which was related with the change of the ebb and flow of antigen.

Comparing sensitivity among IHA, F-ELISA, and Gold nanorod sensor

The serum from rabbits at various infection periods was analyzed by IHA test, F-ELISA, and Gold nanorods sensors. The IHA test could not detect the positive serum from 1 to 3

weeks, but could detect it from 4 to 8 weeks, such positive results are shown as “+”, “++”, and “+++” respectively, and the control group was negative (Table 1). For F-ELISA, the positive serum OD threshold value (0.1068) was 2.1 times of the average OD value (0.0509) of control serum. The results showed that the OD value of positive serum from 1 to 4 weeks were all less than the positive threshold of 0.1068, as was negative serum. From 5 to 8 weeks, the positive serum OD values were greater than 0.1068. Hence, recognition of early infection by analyzing serum with IHA and F-ELISA lacked sensitivity, but these assays can be used to analyze serum in the advanced infection. GNRs sensors can recognize the *S.japonicum* infection in serum from 1 to 8 weeks (Fig. 6).

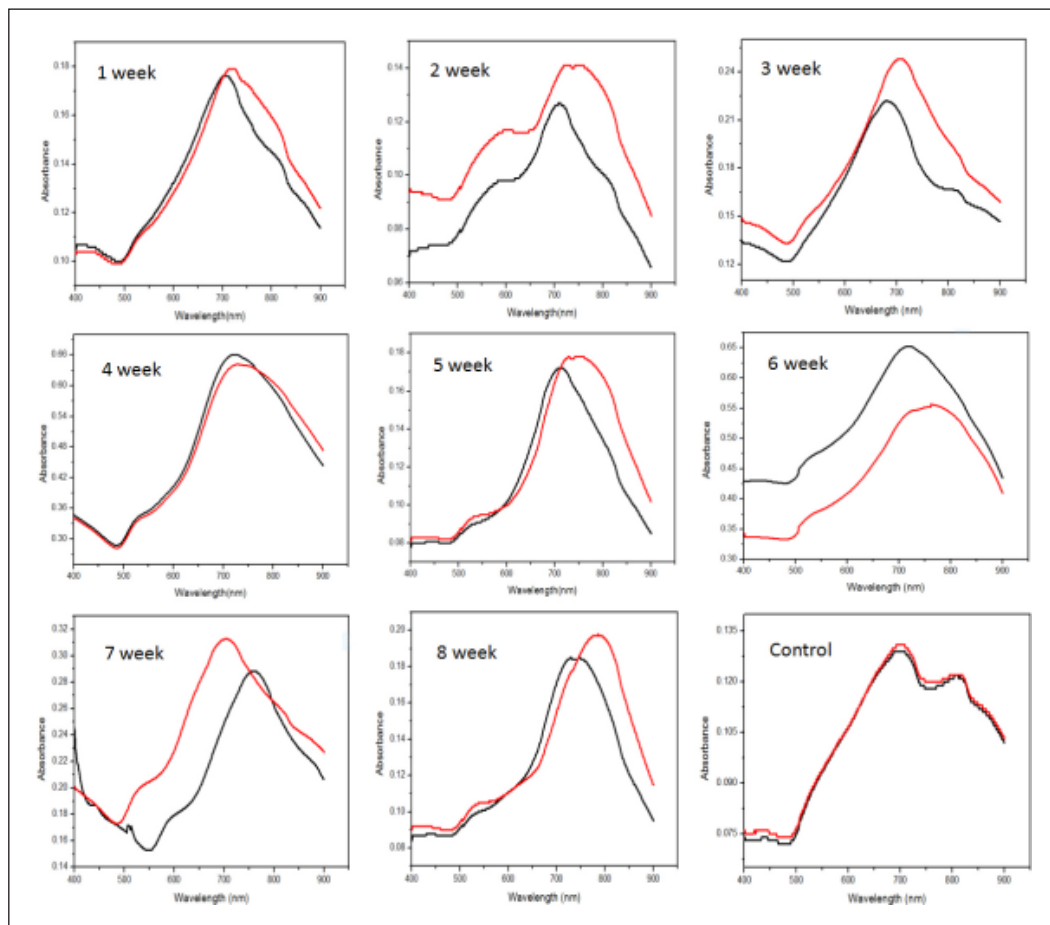


Figure 11. UV-Vis absorption spectra of sensors detect rabbit serum samples infection with *S.japonicum* from 1 to 8 weeks. The displacements of absorption spectra were 12nm, 15nm, 27nm, 5nm, 40nm, 45nm, 53nm, and 57nm, respectively. The control group showed no spectral movement.

Table 1. IHA test the different periods serum infection with *S.japonicum*

| | 1 week | 2 week | 3 week | 4 week | 5 week | 6 week | 7 week | 8 week |
|------|--------|--------|--------|--------|--------|--------|--------|--------|
| 1:10 | - | - | - | + | ++ | ++ | +++ | +++ |
| 1:20 | - | - | - | + | + | ++ | +++ | +++ |
| 1:40 | - | - | - | + | + | ++ | +++ | +++ |
| 1:60 | - | - | - | + | + | ++ | +++ | +++ |

Legend: “+” Positive, “-” Negative.

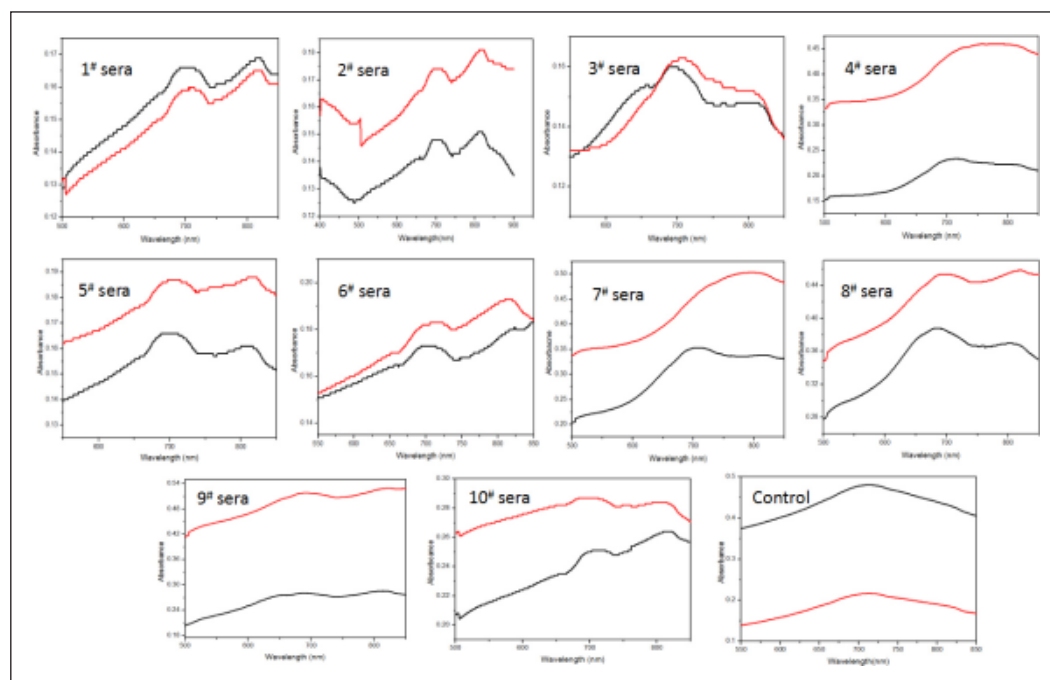


Figure 12. Human serum *S.japonicum* infections were detected by gold nanorod optical sensor. The results show that 10 human serum samples were detected by gold nanorod optical sensor, and the displacement of absorption spectra of nanosensor were 15nm, 12nm, 15nm, 43nm, 9nm, 10nm, 91nm, 19nm, 14nm, and 17nm respectively. Health human serum (control group) showed no spectral movement.

Gold nanorod sensors were also used to detect *S.japonicum* infection in human serum. The results demonstrate that different infection serums have various displacement of LSPR wavelength and the health human serum did not show any displacement (Fig. 12).

DISCUSSION

In this study, we prepared GNRs by seed-mediated growth. ITO glass was chosen as a

substrate, and was modified by hydroxylation and sulfhydrylation, then assembled with the gold nanorods for constructing the solid phase gold nanorods sensor. We combine the SIEA26-28kDaSjscFv on the surface of sensors, based on the specific interaction of SIEA26-28kDaSjscFv with *S.japonicum* circulating antigens to complete the detection. ITO glass was covalently bonded to gold nanorods, which was verified by TEM technology and EDX analysis. However, the absorption spectra of sensors changed during the assembly process, because of the

GNRs in different medium environments showed different refractive index values. A mathematical model proposed by Lee & El-Sayed can be used to explain this phenomenon (Lee & El-Sayed 2006). In this study, as GNRs were placed from the liquid to the ITO-glass, the refractive index (RI) was increased from 1.3 (RI for liquid) to 1.8 (RI of ITO glass). The RI is inversely proportional to the square of the plasma wavelength; therefore, as the medium's refractive index increases, the refractive index of the biosensor decreases. The wavelength of the plasma bands of GNRs is given by the following equation:

$$\lambda_{res} = \lambda_p (\epsilon_b + Yn_m^2)^{1/2} \quad (1)$$

where λ_{res} is the plasma wavelength of GNRs, n_m is the refractive index of the surroundings, λ_p is the plasma wavelength of bulk metal, ϵ_b represents the inter-band contribution of the GNRs to the dielectric function, and Y is a geometric parameter proportional to the square of Aspect Ratio (AR) of GNRs, YAR^2 . Hence, Equation (1) shows that the change in the plasma wavelength of GNRs is influenced by factors such as bulk plasma wavelength, aspect ratio, and refractive index of the local environment.

Rabbits' serum from 1 to 8 weeks after *S.japonicum* infection, which were analyzed by IHA, F-ELISA, and Gold nanorods sensors. We found that gold nanorod sensors could be used to recognize infection at all time points based on the LSPR spectra shifts. From 1 to 3 weeks, the LSPR spectra shifts increased, and then decreased until the fifth week, and the LSPR spectra shifts increase again. Considering the life cycle of *S.japonicum*, we know that the LSPR spectra increases up to the third week due to the cercaria boring into the body and producing the circulating antigen, and as time increases, the immune system starts to fight against the circulating antigen in the body. Therefore, the gold nanorod sensors detected less antigens for the fourth week, so the LSPR spectra displacement also decreased. In the fifth week, many of schistosomula become adults, and mating and ovulation lead to the circulating antigen levels to increase again.

Hence, the LSPR spectra shifts of gold nanorods sensors increased accordingly. Based on these experiments, we attempted to detect *S.japonicum* infection in human serum by gold nanorod sensor, and the results keep consistent with the IHA and F-ELISA test.

The gold nanorods optical sensor makes up for the deficiency of the traditional pathogenic biological and immunological methods, which are not capable of early diagnosis of schistosomiasis, and the new method also provides a new basis for testing other parasitic diseases in early infection stages.

CONCLUSION

This study built a solid gold nanorods optical sensor with high sensitivity, high specificity, and capability to detect circulating antigens of *S.japonicum* in the blood. The findings of this research can be used to detect of schistosomiasis in low epidemic areas. Moreover, the sensor also used for the analysis of serum from schistosomiasis patients, and the sensor is expected to provide a new technology for the early diagnosis and prevention of schistosomiasis.

Acknowledgement. This work was supported by the Key Discipline of Pathogenic Biology and Key Laboratory of immune and control the spread of schistosomiasis in Hunan Province. We would like to acknowledge the National Natural Science Foundation of China for funding this research (Grant number: 81271862).

REFERENCES

- Cai, Y.C., Chen, S.H., Tian, L.G., Chu, Y.H., Lu, Y., Chen, M.X., Ai, L., Zhou, Y. & Chen, J.X. (2014). [Establishment of A1E3 and B1C4 monoclonal antibody-based ELISA for detecting circulating antigen of *Schistosoma japonicum* and its preliminary application]. *Zhongguo Xue Xi Chong Bing Fang Zhi Za Zhi* **26**: 42-45, 89.

- Chen, C.D., Cheng, S.F., Chau, L.K. & Wang, C.R. (2007). Sensing capability of the localized surface plasmon resonance of gold nanorods. *Biosensors & Bioelectronics* **22**: 926-932.
- Chitsulo, L., Loverde, P. & Engels, D. (2004). Schistosomiasis. *Nature Reviews Microbiology* **2**: 12-13.
- Chu, X., Xiang, Z.F., Fu, X., Wang, S.P., Shen, G.L. & Yu, R.Q. (2005). Silver-enhanced colloidal gold metalloimmunoassay for *Schistosoma japonicum* antibody detection. *Journal of Immunological Methods* **301**: 77-88.
- Gao, D.M., Wang, S.P., He, Z., Fung, M.C., Liu, M.S., Yu, L.X. & Chen, X.C. (2010). *Schistosoma japonicum*: screening of cercariae cDNA library by specific single-chain antibody against SIEA26-28 ku and immunization experiment of the recombinant plasmids containing the selected genes. *Parasitology Research* **107**: 127-134.
- Kongs, A., Marks, G., Verle, P. & Van der Stuyft, P. (2001). The unreliability of the Kato-Katz technique limits its usefulness for evaluating *S.mansoni* infections. *Tropical Medicine & International Health* **6**: 163-169.
- Lee, K.S. & El-Sayed, M.A. (2006). Gold and silver nanoparticles in sensing and imaging: sensitivity of plasmon response to size, shape, and metal composition. *Journal of Physical Chemistry B* **110**: 19220-19225.
- Legesse, M. & Erko, B. (2008). Field-based evaluation of a reagent strip test for diagnosis of *schistosomiasis mansoni* by detecting circulating cathodic antigen (CCA) in urine in low endemic area in Ethiopia. *Parasite* **15**: 151-155.
- Lei, J.H., Guan, F., Xu, H., Chen, L., Su, B.T., Zhou, Y., Wang, T., Li, Y.L. & Liu, W.Q. (2012). Application of an immunomagnetic bead ELISA based on IgY for detection of circulating antigen in urine of mice infected with *Schistosoma japonicum*. *Veterinary Parasitology* **187**: 196-202.
- Liu, G.D., Wu, Z.Y., Wang, S.P., Shen, G.L. & Yu, R.Q. (2001). Renewable amperometric immunosensor for *Schistosoma japonicum* antibody assay. *Analytical Chemistry* **73**: 3219-3226.
- Lu, Y., Xu, B., Ju, C., Mo, X., Chen, S., Feng, Z., Wang, X. & Hu, W. (2012). Identification and profiling of circulating antigens by screening with the sera from *schistosomiasis japonica* patients. *Parasites & Vectors* **5**: 115.
- Mayer, K.M. & Hafner, J.H. (2011). Localized surface plasmon resonance sensors. *Chemical Reviews* **111**: 3828-3857.
- Bergquist, N.R. (1992). Immunodiagnostic approaches in schistosomiasis. England: John Wiley & Sons Ltd.
- Shalabney, A. & Abdulhalim, I. (2012). Figure-of-merit enhancement of surface plasmon resonance sensors in the spectral interrogation. *Optics Letters* **37**: 1175-1177.
- Szunerits, S., Maalouli, N., Wijaya, E., Vilcot, J.P. & Boukherroub, R. (2013). Recent advances in the development of graphene-based surface plasmon resonance (SPR) interfaces. *Analytical and Bioanalytical Chemistry* **405**: 1435-1443.
- Wang, S., Yin, T., Zeng, S., Che, H., Yang, F., Chen, X., Shen, G. & Wu, Z. (2012). A piezoelectric immunosensor using hybrid self-assembled monolayers for detection of *Schistosoma japonicum*. *PLoS One* **7**: e30779.
- Wang, Y. & Tang, L. (2013). Chemisorption assembly of Au nanorods on mercaptosilanized glass substrate for label-free nanoplasmon biochip. *Analytica Chimica Acta* **796**: 122-129.
- Wen, Z., Wang, S., Wu, Z. & Shen, G. (2011). A novel liquid-phase piezoelectric immunosensor for detecting *Schistosoma japonicum* circulating antigen. *Parasitology International* **60**: 301-306.
- Wu, Z.Y., Shen, G.L., Wang, S.P. & Yu, R.Q. (2003). Quartz-crystal microbalance immunosensor for *Schistosoma japonicum* - infected rabbit serum. *Analytical Sciences* **19**: 437-440.